We are IntechOpen, the world's leading publisher of Open Access books Built by scientists, for scientists

4,800
Open access books available

122,000
International authors and editors

135M
Downloads

Our authors are among the

154
Countries delivered to

TOP 1%
most cited scientists

12.2%
Contributors from top 500 universities

CLARIVATE ANALYTICS BOOK CITATION INDEX INDEXED

WEB OF SCIENCE™

Selection of our books indexed in the Book Citation Index in Web of Science™ Core Collection (BKCI)

Interested in publishing with us?
Contact book.department@intechopen.com

Numbers displayed above are based on latest data collected.
For more information visit www.intechopen.com

6

Solution Processable Ionic *p-i-n* Organic Light-Emitting Diodes

Byoungchoo Park
Department of Electrophysics, Kwangwoon University, Seoul
Korea

Strong and efficient light emission from organic light emitting devices (OLEDs) fabricated by simple solution process is potentially useful for the manipulation of light in information display and lighting technologies. Recently, intensive research has been conducted into the development of OLEDs for realizing strong light emission from a simple OLED structure. In this chapter, highly efficient and enhanced light emission will be described for solution-processed phosphorescent OLEDs (PHOLEDs) doped with ionic salt, treated with the simultaneous electrical and thermal annealing. Because the simultaneous annealing causes the adsorption of charged salt ions at the electrode surfaces, the separated charges act as ionic doping in organic semiconductor layer and the electronic energy levels of the organic molecules are bended by the electric fields due to the adsorbed charged ions at the electrode interfaces, i.e., the simultaneous annealing can induce the proper formation of ionic *p-i-n* structure.

1. Introduction

Recent research has focused on the development of organic materials and device structures for use in organic light-emitting devices (OLEDs), with the aim of realizing cost-efficient, lightweight, and large–area flat panel displays (Tang & VanSlyke, 1987, Burroughes et al., 1990, Baldo et al., 1998). In order to achieve this aim, the scientific developments of the greatest interest to researchers are the improved efficiency, stability, and simplicity of the device fabrication process. In respect of the efficiency of these devices, for example, their internal quantum efficiency has been improved significantly of late, and is currently typically near 100%, as a result of incorporating phosphorescent dopant into the electroluminescent (EL) layer. This innovation has resulted in strong spin-orbit coupling, which leads to a rapid intersystem crossing and a radiative transition from triplet states to a ground state, thus promoting enhanced EL emissions (Baldo et al., 1998, Baldo et al., 1999, Adachi et al., 2002, He et al., 2004). By making use of the electro-phosphorescent Ir complex, it has been possible to create phosphorescent OLEDs (PHOLEDs) with an increased peak luminescence of up to ~ 50,000 cd/m² (Baldo et al., 1998, Baldo et al., 1999, Adachi et al., 2002, He et al., 2004). In contrast, relatively little progress has been made to date in designing a reliable and simple fabrication process that ensures the formation of a flat and uniform EL layer over a large area, which is particularly important for achieving the highly efficient and reliable device performance that is required for OLEDs. During the fabrication

of OLEDs, the organic layers used are typically prepared using physical vapor deposition (Tang & VanSlyke, 1987, Baldo et al., 1998, Baldo et al., 1999, Adachi et al., 2002, He et al., 2004) or wet solution-coating processes (Friend et al., 1999, Pardo et al., 2000, Jabbour et al., 2001, Ouyang et al., 2002, de Gans et al., 2004, So et al., 2007). To date, OLEDs manufactured using vapor-deposited organic multi-layers of small molecular materials have the best performance record. However, the vapor deposition process is quite complex and expensive. Solution-processed devices made of polymeric or small molecular materials are also of interest, because these techniques make possible a simple production technique that uses a non-vacuum process such as continuous coating, screen printing, and Ink-jet printing (Pardo et al., 2000, Jabbour et al., 2001, Ouyang et al., 2002, de Gans et al., 2004, So et al., 2007). In such solution-processed devices, it is of critical importance to achieve strong light emission from a simple OLED structure. For that purpose, several trials have been made. One of the simplest devices tested is a solution-processed PHOLED (Yang & Neher, 2004, Liu et al., 2005, Niu et al., 2005, Suzuki et al., 2005). Usually, solution-processed PHOLEDs are prepared by doping a low molecular weight phosphorescent dye, such as an iridium complex, into a proper polymer matrix that contains a large-band-gap polymer, such as poly(vinylcarbazole) (PVK) (Yang & Neher, 2004, Liu et al., 2005, Niu et al., 2005). To achieve a better balance of charge transport in these devices, an interfacial layer, such as CsF, LiF, and/or surfactant layer, was also introduced between the phosphor-doped emissive layer and the metal (Al) cathode (Yang & Neher, 2004, Liu et al., 2005, Niu et al., 2005, Park et al., 2007). For a representative example, a power conversion efficiency (η_P) of 24 lm/W at current efficiency (η_C) of 30 cd/A was reported for PHOLEDs with the 1 nm CsF interfacial layer and the Al cathode (Yang & Neher, 2004). Another method is to use a bilayer cathode that consists of an electron-injection layer, such as Ca, Ba, or Cs, and Al evaporated onto the light-emitting polymer layer (Suzuki et al., 2005). A peak η_P of 38.6 lm/W was reported when the bilayer cathode was used (Suzuki et al., 2005). Although such efficient single-layered PHOLEDs with the interfacial layer have been demonstrated, the processes by which PHOLEDs are fabricated remain inadequate; the device structure is still complex and thus the fabrication process is complicated. In order to realize strong light emission from simple OLED devices, another possible method of preparation is to use an organic light emitting layer doped with organic salt (Sakuratani et al., 2001, Lee et al., 2002, Xu et al., 2003). By using fluorescent OLEDs with the doped organic layer and a simple Al cathode, enhanced EL emission was observed after treatment with a high electric field at room temperature (Sakuratani et al., 2001). This device is simple, and hence potentially inexpensive to make. However, there still remain problems regarding inhomogeneous emission, low reproducibility, and undesirable electric field treatment at high field strength over 20 V. Thus, the effect of doping with salt on performance in OLEDs has not yet been fully investigated (Yim et al., 2006). Hence, a new work was initiated to improve the device's high efficiency and brightness further by doping with organic salt and simultaneous treatments of electrical and thermal annealing. It will be shown that the improved device yields homogeneous emission and an increase in EL emission with high reproducibility.

The structure of the single-layered PHOLED used is shown in Figure 1. On a transparent substrate, a transparent indium-tin-oxide (ITO) layer was formed as an anode, over which a single electrophosphorescent EL organic layer was formed and upon which a metal cathode Al layer was then deposited. After the PHOLED was fabricated, it was treated thermally and electrically. It was heated to T°C by a hot plate and then an electric field of V was

applied between the anode and the cathode of the device. When the device began to emit EL light, the field was terminated and then the device was cooled to room temperature. In this process, *T*°C was set to be below the glass transition temperature of the used organic materials and *V* to be below 15 V, to prevent deformation of the EL layer. Electric field treatment at elevated temperatures can induce the charge separation of organic salt towards the electrodes efficiently and homogeneously, even at relatively low voltages. That is to say, at the electrode surfaces, the adsorbed ions (positive ions for the n-doped region and negative ions for the p-doped region) can bend the heights of the lowest unoccupied molecular orbital (LUMO) level and the highest occupied molecular orbital (HOMO) level of the organic molecules near the electrodes. Thus, the electrons and holes can be injected easily into the organic layer through the reduced tunneling barriers from the electrodes. Note that this situation is quite similar to the ion implantation in inorganic semiconductors (Chason et al., 1997, Gerstner et al., 2001). Thus, one may also expect that the simultaneous treatments will be useful for further increasing EL emission from a homogeneous emitting area with high reproducibility.

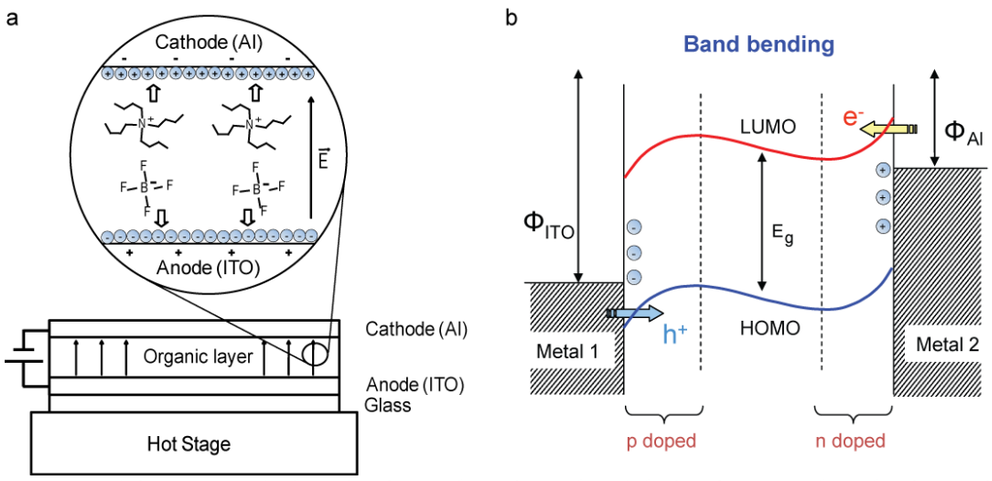

Fig. 1. (a) Architecture of the devices showing the fabrication of the device with the simultaneous electrical and thermal treatments. (b) Schematic energy levels of the device after the simultaneous treatments.

2. Fabrication of solution processable ionic *p-i-n* OLEDs

For the fabrication of devices, glass substrates (0.7 mm) coated with ITO (80 nm, 10-20 ohm/square sheet resistance) were used. After routine cleaning procedures for the substrate with wet (acetone and isopropyl alcohol) and dry (UV-ozone) processes, a blended solution of organic materials was spin coated (700 rpm) on top of ITO, precoated with a poly(3,4-ethylenedioxythiophene) : poly(4-styrenesulphonate) (PEDOT:PSS) hole-injecting buffer layer. The basic organic solution consisted of a hole transporting material of N,N'-diphenyl-N,N'-bis(3-methylphenyl)-1,1'biphenyl-4,4'-diamine (TPD: 0.08 wt%), an electron transporting material of 2-(4-biphenylyl)-5-(4-tert-butylphenyl)-1,3,4-oxadiazole (Bu-PBD: 0.32 wt%), a green emitting material of tris(2-phenylpyridinato) iridium ($Ir(ppy)_3$: 0.06 wt%), and a hole-transporting host material of PVK (0.34 wt%) into mixed solvents of 1,2-dichloroethane and chloroform (mixing weight ratio 3:1), which have different volatilities.

The organic salt of tetrabutylammonium tetrafluoroborate (Bu_4NBF_4) was further dissolved into the basic organic solution at an appropriate concentration. The thickness of the spin-coated organic layer was about 80 nm. Then, an Al cathode layer (100 nm) was formed on the top of the organic layers via thermal deposition at a rate of 0.7 nm/s under a base pressure of 2×10^{-6} Torr. In this experiment, phosphorescent OLEDs were fabricated and compared: one with Bu_4NBF_4 (0.0050 wt%) annealed electrically at V = +7 V (forward bias) at T = 65°C; the other for reference with Bu_4NBF_4 (0.0050 wt%) annealed electrically at V = +20 V (forward bias) at T = 25°C. It should be noted that, except for the emissive layer, the device structure of the reference device was identical to that of the sample device. The structures of the devices and materials used were identical. The devices were prepared in inert Ar gas environments; this preparation included electrical and thermal treatments.

3. Ionic *p-i-n* PHOLEDs made by spin-coating

3.1 Performance of ionic *p-i-n* PHOLEDs with a structure of [ITO / PEDOT:PSS / EL layer / Al]

First, the current flows were observed for sample and reference devices doped with Bu_4NBF_4 during the electric field treatment under given temperature. Figure 2 shows the plots of the current flows of the devices for the applied voltage profiles, which are shown in the inset of the figure. As shown in the figure, the current flow of the sample device was 2.1 mA/cm² at t = 0 s (before annealing) and increased to 12.4 mA/cm² at t = 33 s (after annealing), while that of the reference device was 63 mA/cm² at t = 0 s (before annealing) and increased abruptly to 730 mA/cm² at t = 4.5 s (after annealing). The figure shows clearly the smooth increase in current flow of the sample device with time during the simultaneous treatments. This smooth increase means that the organic salt ions that have been separated by the electric field move slowly towards the interfaces of the electrodes at elevated temperature and the accumulated ions near the interface reduce the interfacial barriers for carrier injection between the electrode and the organic layer, which may lead to improved electrical characteristics of the sample device. By comparing this smooth increase with the abrupt current increase of the reference device during the electrical treatment, one can see clearly that the increase in current flow of the sample device was smaller than that of the reference device. Thus, the deterioration of the reference device due to the abrupt increase in current flow through the organic layer under high voltage will be prevented by application of the simultaneous treatments. Thus one can easily fabricate sample devices with high reproducibility by applying the simultaneous treatments under low voltage. Note that during the treatment, one can see the current spikes at the rising edges of squared waveform for the sample device. These spikes may be due to the reduction of capacitance by the separated ions near the electrode surface.

Next, we observed the EL operation of the sample and reference devices with the naked eye. Figure 3 shows a photograph of the operating sample and reference devices. For clear comparison, we took a photograph of the device operation under different bias. The figure clearly demonstrates that all across the active areas, there is bright and homogeneous EL emission from the 3 × 3 mm² active area in the sample device, while relatively small and inhomogeneous emission was observed in the reference device even under higher bias. Similar to the current flows, it is also noted that the sample device exhibited much greater reproducibility than the reference device. We also observed the EL spectra for sample and

reference devices (Fig. 3 (b)). As shown in the figure, the spectra are almost identical to those for the multilayered PHOLEDs reported previously (Baldo et al., 1999); there is an emission peak wavelength of 516 nm with full width at half maximum (FWHM) of ~70 nm. These results for the spectra indicate clearly that the doped organic salt does not disturb the EL spectrum, i.e., the energy levels of the organic material emitting layer. Note that the Commission Internationale de L'Eclairage (CIE) coordinates of (x=0.296, y=0.631) for the device and the EL spectrum are independent of current density.

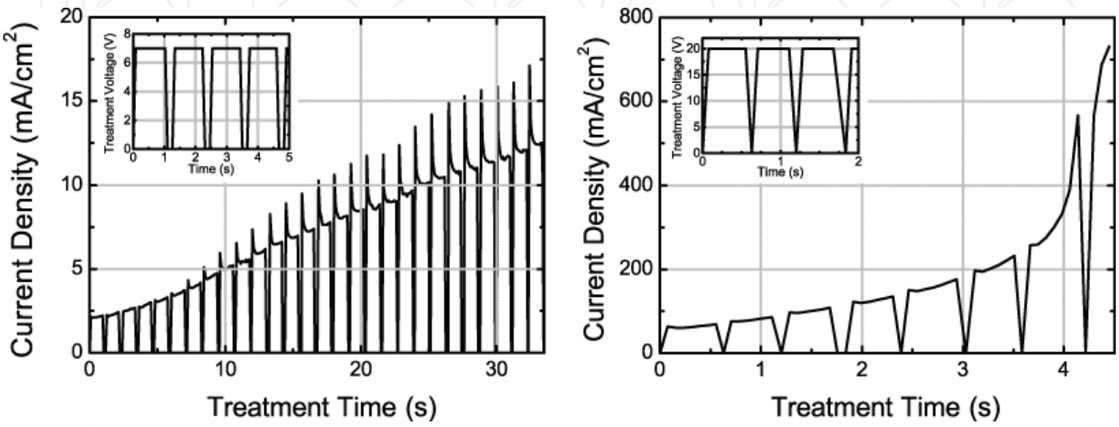

Fig. 2. Current flows of sample (left) and reference (right) devices with organic salt during electrical and thermal treatments for given temperatures. The inset shows the voltage profile applied to the devices. (Oh et al., 2007)

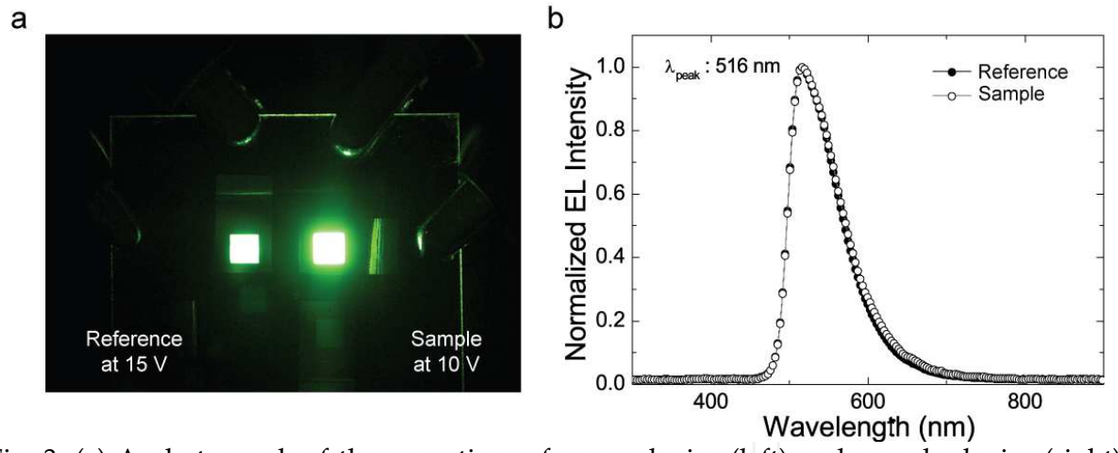

Fig. 3. (a) A photograph of the operating reference device (left) and sample device (right). The active area of each PHOLED is 3 × 3 mm^2. (b) The normalized EL spectra for the operating sample device (open circles) and reference device (closed circles). (Oh et al., 2007)

Next, in order to understand the effect of the organic salt, we observed the dependence of the EL characteristics on the doping concentration of the salt for the sample device, treated at V = +7 V (forward bias) and T = 65°C. Figure 4 (a) shows the current density-voltage (J-V) characteristics of the treated devices for various concentrations of Bu_4NBF_4. The rate of increase of the current density increases as the doping concentration increases. For the doped PHOLEDs, the current density behaves according to the power law equation of J =

$k \cdot V^{m+1}$ (Burrows & Forrest, 1994, Brutting et al., 2001) (where k is a proportional constant and m is 4 for doped devices, while m is 3 for an undoped device). This indicates that the space charge limit current (SCLC) due to the traps increases as the doping concentration increases. The luminance-voltage (*L-V*) characteristics of the devices are shown in Fig. 4 (b). As the doping concentration increases from zero, the EL luminescence also increases greatly. As shown in the figure, for the sample device with a doping concentration of 0.0050 wt%, the low turn-on voltage (2.5 V for 1 cd/m²) and a steep increase in the *L-V* curve under low *J-V* characteristics suggest that both holes and electrons can easily be injected into the organic layer. The operating voltage for a typical display application is 4.2 V to obtain a brightness of 100 cd/m² (0.48 mA/cm²) and 6 V for 1,000 cd/m² (3.47 mA/cm²); the luminescence reached ~51,000 cd/m² (at 13.5 V), which is two orders of magnitude higher than that (~426 cd/m²) of the device with 0 wt% concentration. Note that the EL properties of devices without any thermal/electrical annealing were exactly the same as those of the 0 wt% sample. Note also that the luminance of the device was comparable to that of the previously reported EL device (22,100 cd/m² at 10 V) fabricated with a CsF interfacial layer and Al cathode (Yang & Neher, 2004).

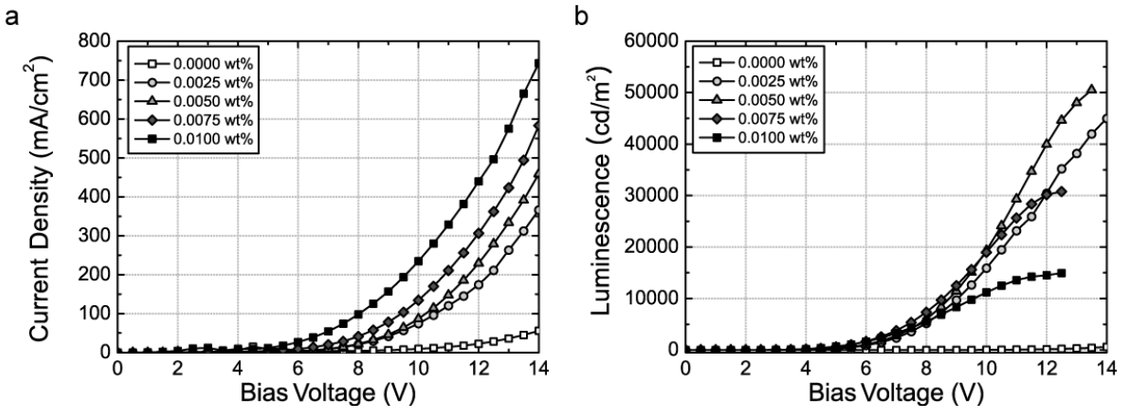

Fig. 4. Characteristics of *J-V* (a) and *L-V* (b) for the single-layered $Ir(ppy)_3$ PHOLEDs with various concentrations of Bu_4NBF_4. (Oh et al., 2007)

Here, it is noted that the enhanced EL emission caused by the adsorption of ions at the electrode surface for the salt-doped PHOLED treated by the thermal and electrical annealing. At the ITO anode contact, the accumulation of separated negative BF_4^- ions can assist hole injection from ITO to the organic layer and an Ohmic contact is achieved at the ITO interface (Sakuratani et al., 2001). At the same time, the accumulation of the positive Bu_4N^+ ions near the cathode aids the injection of electrons from the metal cathode into the organic layer by reducing the tunneling barrier of the cathode interface. Thus, proper adsorption of ions at the interfaces between the organic layer and the electrodes can enhance the injection of charge carriers into the organic layer, which results in the enhancement of current flow (SCLC) and EL luminance.

Next, the sample ionic *p-i-n* PHOLEDs was compared with typical (frozen) light-emitting cells (LECs) (Pei et al., 1995, Gao et al., 1997, de Mello et al., 1998). In LECs, the organic salt is also doped into the light-emitting polymer layer to improve the device performance. However, there are five main differences between typical LECs and the sample devices presented in this

study. 1) In typical LECs, an ionic conducting material, such as poly-(ethylene oxide) (PEO), is required. However, in the sample devices presented in this study, no ionic conducting material is necessary, even though the active organic layer used in the sample device has very low ionic mobility. 2) The characteristics of the sample devices depend strongly on the thickness of active layer, in contrast to the LECs (Pei et al., 1995, Gao et al., 1997, deMello et al., 1998). 3) The forward- and reverse-biased *J-V* and *L-V* curves of the typical LECs were almost symmetric about zero bias, in contrast to the diode-like behaviors exhibited in the sample devices. 4) The polarity of the *p-i-n* junction of the sample device cannot be switched by reversing the polarity of the electric field at elevated temperature, in contrast to the polarity of the frozen junction LECs, which is dictated by the polarity of the prebias at high temperature (Gao et al., 1997). These results mean that it is only for forward simultaneous treatments (Al connected as the cathode) that electrons and holes are injected efficiently from the electrodes to recombine in the organic EL layer to generate photons, in contrast to the typical frozen LECs. 5) The dynamic response of the typical LECs was determined by the ionic mobility. Thus, the response time depended on whether the PEO ion-transport polymer was added (~1 s) or not (~60 s) to the polymer blend. However, the dynamic response (~10 μs) of the sample device is determined by mobility of the charge carrier (electron and hole). It will thus be evident that our device is quite different from typical LECs. The fast response time of the sample device also clearly indicates that the ions separated by the simultaneous treatments remain at the contacts in a stable fashion and the ions at the interfaces enhance the charge injection into the organic layer.

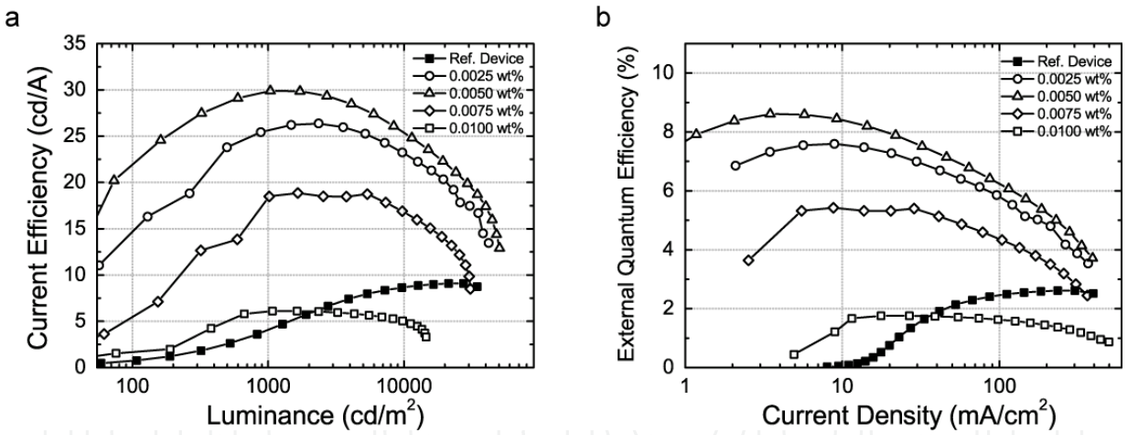

Fig. 5. Current efficiency (η_C) vs. luminance (a) and external quantum efficiency (η_{ext}) vs. current density (b) of the single-layered $Ir(ppy)_3$ sample devices (open symbols) with various concentrations of Bu_4NBF_4 and reference device (closed square). (Oh et al., 2007)

Next, in order to confirm the effect of the simultaneous annealing, we also investigated the efficiency characteristics of the sample devices. Fig. 5 (a) shows the current efficiency-luminance (η_C-*L*) of the PHOLEDs. As shown in the figure, PHOLEDs (0.0050 wt%) after the annealing treatments are more efficient than the reference device: for the sample device, η_C of 22 cd/A was obtained at 100 cd/m^2, reaching η_C = 30 cd/A at 1000 cd/m^2, while for the reference device, η_C of 0.7 cd/A at 100 cd/m^2, and η_C = 4 cd/A at 1,000 cd/m^2. We also observed the external quantum efficiency η_{ext} of the sample devices. Here, η_{ext} was determined from the conventional luminance-current characteristics of the EL spectrum

(Okamoto et al., 2001). As shown in Fig. 5 (b), η_{ext} of the sample device (0.0050 wt%) is much higher than that of the reference device: for the sample device, η_{ext} increases, reaches a maximum of 8.6 %, and then slowly decreases with increasing current density, while for the reference device, η_{ext} reaches only a maximum of 2.6 %. For another comparison, η_{ext} s of 8 ~ 12 % of the hetero-structured PHOLEDs, reported in References (Baldo et al., 1999, Adachi et al., 2002), are comparable to that of the sample device. These results indicate clearly that the charge balance in the charge injection was improved significantly by controlled adsorption of ions at the interfaces.

Therefore, by applying electric and thermal treatments simultaneously, homogeneous and enhanced EL emission was obtained from the active area of the devices with high reproducibility. Moreover, the efficiency of the devices was also observed to improve. As a result, an ionic *p-i-n* PHOLED with a peak external quantum efficiency of 8.6 % was achieved in the sample device. On the basis of these results, it is demonstrated that simultaneous annealing can lead to more efficient electroluminescence through increased and balanced carrier injection. This improvement can be attributed to the excellent balancing of holes and electrons.

3.2 Performance of PHOLEDs with a structure of [ITO / EL layer / CsF / Al]

Although efficient solution-processed PHOLEDs have been demonstrated, the process of their fabrication is still complex because a hole injecting buffer layer of PEDOT:PSS has been introduced between the emissive layer and the transparent ITO anode. Given the state of research, a new work was initiated to achieve high efficiency and brightness from the simplest PHOLED structure that it is possible to achieve. In order to realize strong light emission from a real single-organic-layered PHOLED, a modified PHOLED was proposed by including an ionic salt-doped emissive layer, treated by appropriate simultaneous electrical annealing at elevated temperature.

The proposed device structure is very simple; on a glass substrate, an ITO layer was formed as an anode, over which an electro-phosphorescent EL layer doped with organic salt was formed by a solution-process and upon which a metal cathode was deposited. After fabrication, the PHOLED was treated by simultaneous annealing by applying an electric field of V at elevated temperature of T. Then, the ions that separate and accumulate at the electrode surfaces as a result of the treatments induce the electric fields, which can bend the electronic energy levels of organic molecules, enhancing the charge injection into the organic layer from the electrodes across the whole area of the device.

For the experiments, an organic solution consisted of a hole injecting material of 4,4',4"-Tris(N-3-methylphenyl-N-phenyl-amino)-triphenylamine (m-MTDATA), a hole transporting material of TPD, an electron transporting material of Bu-PBD, a green emitting material of $Ir(ppy)_3$, and a hole-transporting host material of PVK at an appropriate concentration into mixed solvent of 1,2-dichloroethane and chloroform. The organic salt, Bu_4NBF_4, was also dissolved into the organic solution. The spin-coated organic layer was about 80 nm thick. Then, a cathode layer of CsF (1 nm) / Al (100 nm) was formed on the top of the organic layers via thermal deposition at a rate of 0.7 nm/s under a base pressure of 2×10^{-6} Torr. In this experiment, the following PHOLEDs were fabricated and compared: annealed sample devices with Bu_4NBF_4 (0.0050 wt%) at V = +9 V (forward bias) at T = 65°C, and, as references, other annealed devices that were not doped.

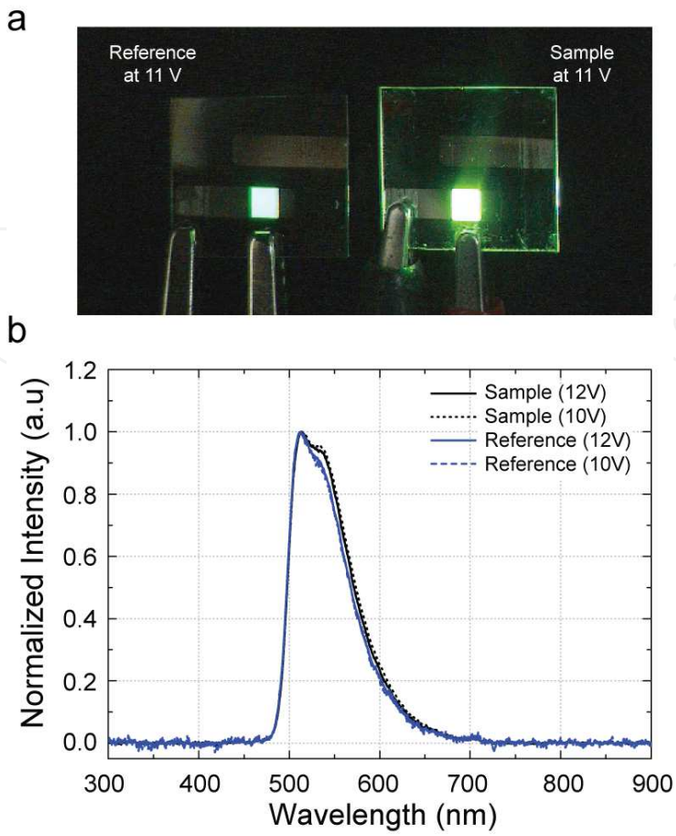

Fig. 6. Upper: A photograph of the operating sample device (right) and reference device (left). Lower: Normalized EL spectra for the operating sample device and reference device. (Park et al., 2008)

The EL operation was observed for the fabricated devices with the naked eye. Figure 6 (a) shows a photograph of the operating devices. For clear comparison, we took a photograph of the device operation under the same bias of 11 V. The figure clearly demonstrates that there is bright and homogeneous EL emission from the active area in the sample device, while there is relatively weak emission from the active area in the reference device. Next, we observed the EL spectra of the devices. As shown in Fig. 6(b), the emission spectra of the sample devices are almost identical to those of the reference devices; there is a spectral peak wavelength of 516 nm with FWHM of ~70 nm. These results for the EL spectra indicate that the doped organic salt does not interfere with the energy band gap of the organic materials. It is likely that the slight increase in the shoulder luminescence near 530 nm for the sample device arises from the more phosphorescent sites at the excited energy level (Xie et al., 2001). It is noted that the CIE coordinate of (x=0.32, y=0.62) for the sample devices is independent of current density. Next, we observed the dynamic responses of the operating devices. As shown in Fig. 7, the observed dynamic responses of the sample device are nearly identical to those of the reference device; the rising time and falling time are about 10 μs and 9 μs, respectively. These fast responses of the sample device indicate that the separated ions remain at the contacts in a stable fashion and the ions at the interfaces can increase the charge injection into the organic layer. In other words, at the ITO anode contact, the

accumulated negative BF_4^- ions can bend the energy level and reduce the tunneling barrier of the anode interface, while the positive Bu_4N^+ ions at the cathode aids the injection of electrons into the organic layer by reducing the tunneling barrier of the cathode interface.

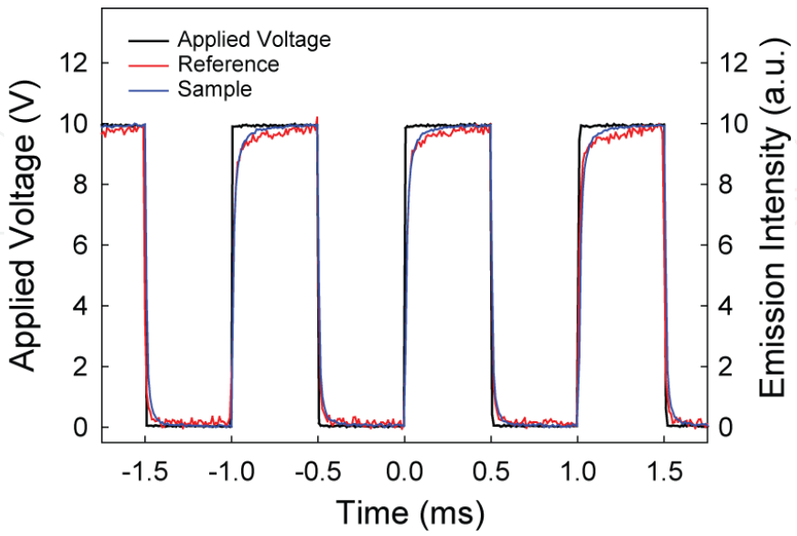

Fig. 7. The dynamic responses for the operating sample device and reference device. (Park et al., 2008)

Next, in order to determine the optimal conditions of operation of the sample device, the dependence of the device characteristics on the concentration of the doping salt has been observed. Figure 8(a) shows The *J-V* characteristics of the sample devices for several concentrations of the salt. As shown in the figure, the rate of increase of the current density increases as the doping concentration increases. The *L-V* characteristics of the devices are shown in Fig. 8(b). As the doping concentration increases from zero, the EL luminescence also increases. The low turn-on voltage (2.5 V for 1 cd/m^2) with a sharp increase in the *L-V* curve even under low current density suggests that both holes and electrons can easily be injected into the annealed organic layer for a doping concentration of 0.0075 wt%, giving ionic concentration of about 10^{19} ~ 10^{20} cm^{-3}. The operating voltage is about 4 V to obtain a brightness of 100 cd/m^2 and about 7 V for 1,000 cd/m^2; the luminescence reached ~35,400 cd/m^2 (at 17.5 V), which is almost three times higher than that (~13,000 cd/m^2) of the reference device. Note that the luminance of the sample device was also comparable to that of a previously reported PHOLED device (Yang & Neher, 2004) that was fabricated with a hole-injecting PEDOT:PSS layer. Thus, it is clear that the proper adsorption of ions at the electrode surface can result in the formation of the ionic *p-i-n* structure and enhance the injection of charge carriers into the organic layer, which results in the enhancement of current flow and EL luminance. To confirm the high performance of the devices, the efficiency was deduced for the studied devices. For the sample device (0.0025 wt%), η_C of 37 cd/A was obtained at 100 cd/m^2, reaching η_C = 34 cd/A at 1,000 cd/m^2, while for the reference device, η_C of 6.5 cd/A at 100 cd/m^2, and η_C = 10.4 cd/A at 1,000 cd/m^2. η_P was also obtained for the sample device; η_P reaches a maximum of 42 lm/W, while for the reference device, η_P reaches only a maximum of 2.8 lm/W. For another comparison, η_Ps of ~30 lm/W of the hetero-structured PHOLEDs, reported in References (Baldo et al., 1999,

Adachi et al., 2002), are comparable to that of the sample device. These results indicate clearly that the balance in the charge injection due to the ionic *p-i-n* structure was improved significantly by controlled adsorption of ions at the interfaces.

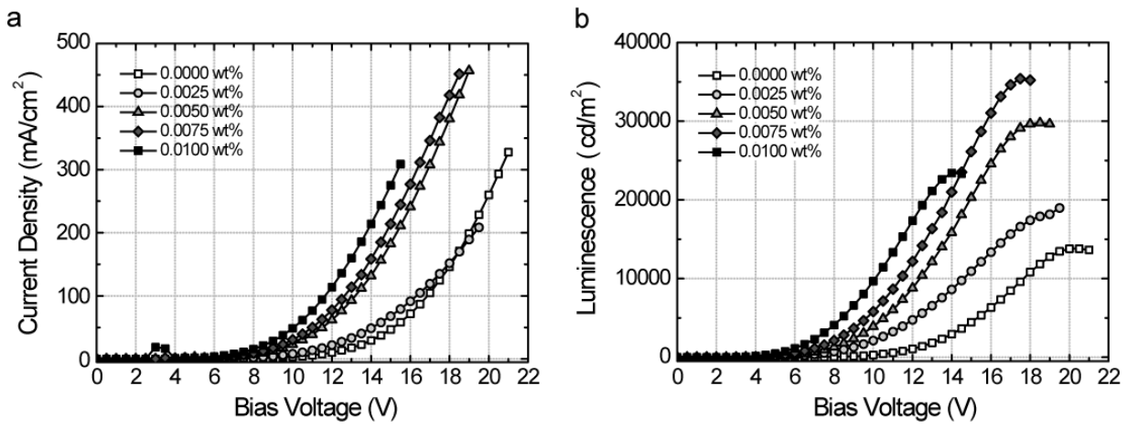

Fig. 8. Characteristics of *J-V* (a) and *L-V* (b) for the single-layered ionic *p-i-n* PHOLEDs with various concentrations of doped salt of Bu_4NBF_4. (Park et al., 2008)

Therefore, herein, a solution-processed single-layered ionic *p-i-n* $Ir(ppy)_3$ PHOLED has been demonstrated. By applying the simultaneous thermal and electrical annealing, homogeneous and enhanced EL emission with increased brightness and high efficiency can be obtained from the devices in a simple fashion. As a result, an ionic *p-i-n* PHOLED with peak power efficiency over 40 lm/W was achieved by means of increased and balanced carrier injections. Given that this device can be fabricated by a simple wet process, combining simultaneous annealing with the use of highly luminous organic materials will surely lead to highly efficient ionic *p-i-n* OLED devices.

4. Ionic *p-i-n* PHOLEDs made by Horizontal-dipping

4.1 Horizontal-dipping method for large area PHOLEDs

For solution-processed devices, spin-coating has until now been the most popular method of forming organic layers. This method is convenient, but has several disadvantages, such as the high stress caused by the spinning motion, the poor uniformity at the edges of large areas, and the large amounts of wasted solution (Pardo et al., 2000, Jabbour et al., 2001, de Gans et al., 2004, So et al., 2007, Tseng et al., 2008). These factors make spin-coating unsuitable for application to large active areas. An alternative method for depositing the solution is to use such techniques as screen printing (Pardo et al., 2000, Jabbour et al., 2001), ink-jet printing (de Gans et al., 2004), or blade coating (Tseng et al., 2008). By using these techniques, organic or polymeric layers may be formed on substrates in a controlled fashion. However, despite the recent developments in such solution-processed devices, an alternative solution-coating process is nevertheless required, because of the continued difficulty of controlling the uniformity of the organic semiconducting layers resulting from the conventional coating methods that have so far been proposed. Hence, further research on solution deposition techniques is required in order to achieve simpler and more reliable fabrication of efficient OLEDs.

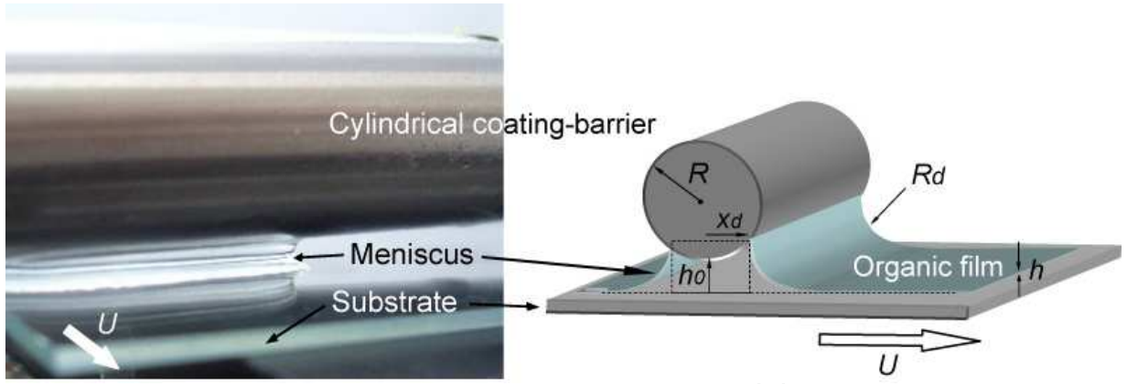

Fig. 9. A photograph (left) with schematic illustration (right) of the premetered horizontal-dip (H-dip) coating process described herein: a cylindrical coating barrier (SUS steel) with a diameter R, a gap height h_0, and a carrying speed U. (Park & Han, 2009)

The advantage of using premetered coating is that the coating thickness is predetermined, in contrast to more typical metered methods such as fixed-gap blade, knife, or wire-bar coatings. Recently, there was a report describing a solution-processed, highly efficient polymer solar cell that was fabricated using a premetered solution-process (Park & Han, 2009). In the study described herein, this premetered process was used to demonstrate the fabrication of efficient, high-performance solution-processed ionic *p-i-n* PHOLEDs.

4.2 Operating principle of H-dipping

It is well-known that coating flows can be divided into two categories, metered or premetered, according to whether the thickness of the coated film is determined by the process or imposed externally. The thickness of the film coated by the metered process is independent of the capillary number, while that produced by premetered process usually increases with increasing capillary number ($C_a=(\mu U/\sigma)$), where μ and σ represent the viscosity and surface tension of the coating solution, respectively, and U is the carrying (coating) speed. Examples of premetered coating flow include meniscus and dip coatings. A photograph and schematic illustration of the premetered solution coating process under investigation are shown in Figure 9. This figure shows a cylindrical coating barrier hanging at a specific height (h_0) above a rigid substrate laid on a carrying stage that transports the substrate in a horizontal direction. The coating process occurs in the following sequence. (1) The substrate is attached to the carrying stage, and the coating barrier is placed at the front edge of the substrate. A blended organic semiconducting molecular solution is then introduced into the empty space between the barrier and the substrate by capillary action, so that a uniform meniscus of the solution may be formed on the substrate by attraction to the barrier (i.e. by surface tension). (2) The substrate is then transported horizontally at constant velocity whilst maintaining the shape of the downstream meniscus. A thin solution layer of the downstream meniscus is then spread evenly on the substrate. While the substrate is being transported, the blended organic solution may be supplied into the gap space at an appropriate injection rate. (3) Having been spread on the substrate, the wet film is dried, and a heater may be used to assist the evaporation of the residual solvent in the wet film on the substrate. Following this process, it is possible to obtain a substrate coated with a solid organic film of uniform thickness. The transport of the substrate through the meniscus of the

solution is similar to that which occurs in the typical dip-coating method (Landau & Levich, 1942, Krozel et al., 2000). In that method, the substrate is immersed in the coating solution and a wet layer is then formed by withdrawing the substrate vertically through the meniscus of the coating solution. Our proposed coating method differs from the conventional dip-coating method, however, because the wet film is formed by withdrawing the substrate horizontally. Therefore, we call the proposed process horizontal dipping (H-dipping) (Park & Han, 2009). It is noted that the apparatus of H-dipping is similar to that of the zone casting (Yabu & Shimomura 2005, Miskiewicz, 2006, Duffy, 2008), that has been used in fabrication of organic transistors, but the coating speed of the zone casting is extremely low (several μm/s) compared with the premetered H-dipping (several cm/s).

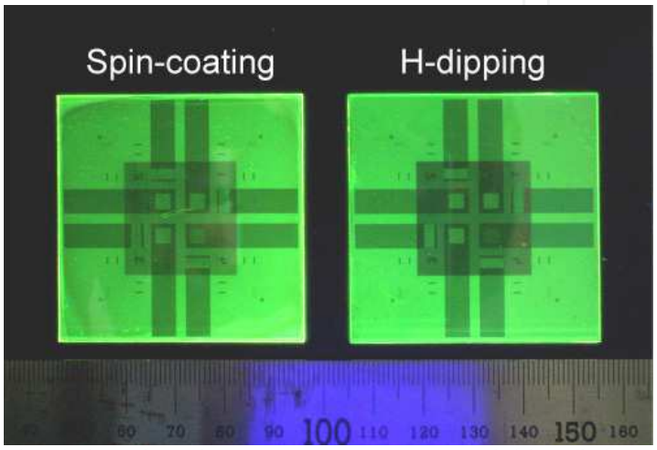

Fig. 10. A photograph of the photoluminescent spin-coated film (left, at 1000 rpm) and the H-dip-coated film (right) on pre-patterned 2" substrates. (Park & Han, 2009)

Photoluminescence images obtained from spin- and H-dip-coated organic films on 2-inch glass substrates (pre-patterned ITO) using a UV light source of 365 nm is shown in Figure 10. It may be seen from the figure that the luminescent intensity and thickness of the spin-coated films vary near the edges of the substrates due to the Bernoulli effect (Luurtsema, 1997). In order to produce a fully smooth spin-coated film, the speed of rotation must be adjusted and the amount of spreading solution increased. On the other hand, it may be seen that the H-dip-coated film is very smooth and uniform. Variation in the thickness of the film was observed only at the very rear edge of the substrate. The surface morphology investigation using AFM showed clearly that the topography was fairly uniform, the root mean square roughness for the H-dip-coated film being only ~0.9 nm, which was comparable to that (~1.0 nm) of the spin-coated films. Moreover, the surface roughness of the H-dip-coated films was identical at different positions. This uniformity was achieved because no external centrifugal force was applied during the formation of the film. Thus, compared to spin-coating, it is possible to achieve uniformity in the film thickness of the EL layer in a reliable way when using H-dipping, even on a large-area substrate. This is a result of the control of the undesirable free-surface flow that occurs at the top organic solution-air interface, via the surface tension effect between the solution and the coating barrier.

The film thickness that results from the H-dipping process may be explained by the description of the associated drag-out problem suggested by Landau and Levich (Landau & Levich, 1942). Based on their description, for a small capillary number (C_a << 1), a useful relationship may be obtained that relates the thickness of the film emerging from a coating bead to the radius of the associated meniscus and carrying speed, U (Landau & Levich, 1942, Park & Han, 2009):

$$h = 1.34\left(\frac{\mu U}{\sigma}\right)^{2/3} \cdot R_d, \quad n \cdot R_d = \left(\frac{x_d^2}{2R} + 2h_0\right) - h, \tag{1}$$

where R_d represents the radius of curvature of the downstream meniscus. Here, R and h_0 represent the radius of the cylindrical coating barrier and the minimum gap height, respectively, and n is 1 for a contact angle of 90° or 2 for a contact angle of 0° measured on the contact line at the interface between the solution and the coating barrier. In our study, n was assumed to be 2, as shown in the photograph (Fig. 9).

It is worthy of note that the thickness of the H-dip-coated film is much less than the gap height. This is characteristic of the main way in which the premetered H-dipping process differs from the conventional metered doctor-blade (or wire-bar) coating (Kuo et al., 2004). In the conventional approach, the doctor-blade (or wire-bar) coating process produces a film thickness of the order of the gap size whose thickness is independent of the carrying speed of the substrate. In the H-dipping method, the premetered process allows the critical control of the thickness and can produce superior quality and extremely thin films at line speeds of the order of a few meters per minute.

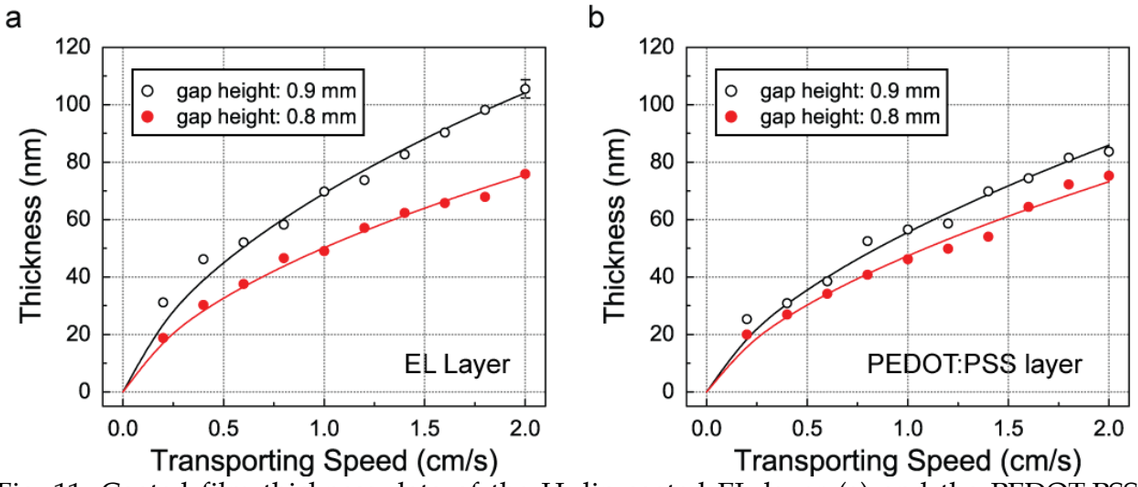

Fig. 11. Coated film thickness data of the H-dip-coated EL layer (a) and the PEDOT:PSS layer (b) as a function of carrying speed for two gap heights (0.9 and 0.8 mm). The solid curves show the theoretical predictions of the Landau & Levich equation. (Park & Han, 2009)

4.3 Fabrication of *p-i-n* PHOLEDs made by H-dipping

For the fabrication of devices, the PEDOT:PSS and the organic EL layers were successively deposited by H-dipping on an ITO-coated glass substrate. The PEDOT:PSS solution used was a mixture of 1 % PEDOT:PSS solution (CLEVIOS™ P VP AI 4083, H.C. Starck) and isopropyl alcohol with a weight ratio of 2:1. The viscosity of the mixed PEDOT:PSS solution, measured by viscometer (RVDV Ⅱ+, Brookfield Inc.), was about 11.6 cp. For the blended EL solution, we used TPD, Bu-PBD, $Ir(ppy)_3$, and PVK without further purification, in mixed solvents of 1,2-dichloroethane and chloroform (3:1). The organic salt, Bu_4NBF_4, was also dissolved into the EL solution. The viscosity of the EL solution was about ~1.0 cp at a temperature of 25°C. The apparatus used for H-dipping had a maximum work space of 15 × 15 cm^2. A small volume of the solution (~ 6 μl) per unit coating area (1 × 1 cm^2) was fed into the gap between the cylindrical barrier (SUS steel, R = 6.35 mm) and the glass substrate using a syringe pump (Pump Systems Inc. NE-1000). The height of the gap, h_0 was adjusted vertically using two micrometer positioners, and the carrying speed U was controlled using a computer-controlled translation stage (SGSP26-200, Sigma Koki Co., Ltd). After a meniscus had formed on the solution, the substrate was transported horizontally, so that the barrier spread the solution on the transporting substrate. The transporting speed U was 1.5 cm/s. It took 2 seconds to prepare a complete film on a substrate with an area of 1.8 × 2.0 cm^2. The H-dip-coated PEDOT:PSS layer and electrophosphorescent EL layer doped with Bu_4NBF_4 were then dried using a heating plate at 110°C for 60 minutes and at 60°C for 5 minutes, respectively, in order to remove the remaining solvents. 1 nm CsF and 60 nm of Al were evaporated sequentially on the EL layer via thermal deposition (0.5 nm/s) at a base pressure below 2 × 10^{-6} Torr. The PHOLED fabricated thus had a device configuration of ITO/ PEDOT:PSS/ EL layer/ CsF/ Al. In the experiment, the sample PHOLEDs with Bu_4NBF_4 (0.0050 wt%) were annealed at V = +8 V (forward bias) at T = 75°C.

4.4 Performance of *p-i-n* PHOLEDs made by H-dipping

By using the AFM, we investigated the dependence of the film thickness, h of the H-dip-coated organic/polymer layer on the transporting speed U and the gap height h_0. The results obtained are shown in Figure 11. As shown in the figure, for a gap height, h_0 of 0.8 mm, the thickness of the H-dip-coated layer increases continuously as the speed U increases in the observed region (filled circles). Furthermore, when h_0 was increased from 0.8 mm to 0.9 mm, the thickness of the H-dip-coated layer also increased with increasing speed U. These results may be explained by the description of the associated drag-out problem, using Equation (1). The theoretical curves resulting from Equation (1) are shown in the figure as solid lines. The observed data fitted the theoretical values predicted by Equation (1) rather well, indicating that the thickness of the H-dip-coated organic film may be controlled by adjusting the gap height h_0 and the carrying speed U. These results indicate that the H-dipping process can be used to produce an organic layer at least as well as spin-coating can. It is further evident that the thickness of the H-dip-coated layer follows nearly the same trends as those shown in previous results using the H-dip-coated photovoltaic layer (Park & Han, 2009).

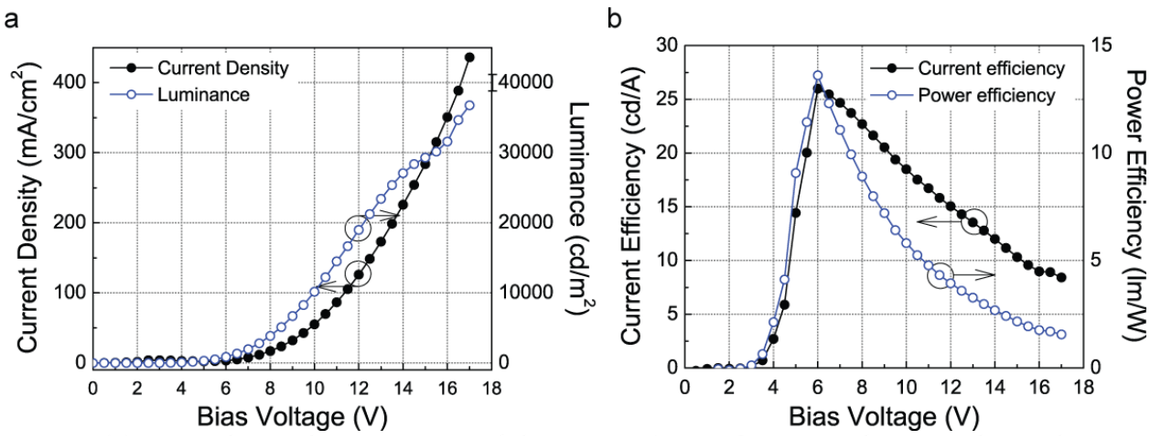

Fig. 12. (a) *J-V* and *L-V* characteristics of the ionic *p-i-n* PHOLED made using the H-dipping process. (b) η_C-*V* and η_P-*V* characteristics of the studied PHOLED.

We then investigated the EL characteristics of the ionic *p-i-n* PHOLEDs produced by the H-dipping process. In the device, the thicknesses of the PEDOT:PSS and the EL layers were adjusted to about 40 nm and 80 nm, respectively. Figure 12(a) shows the observed *J-L-V* characteristics of the fabricated ionic *p-i-n* PHOLED after the simultaneous treatments at T = 75°C and V = +8.0 V. The slope of the *J–V* curve between 0 and 18 V shows the excellent diode behavior of the fabricated OLED and thus indicates good coverage of the H-dip-coated PEDOT:PSS buffer layer and the EL layer. It is clear from the *J-L-V* curves that both the charge injection and turn-on voltages are below 2.7 V, with sharp increases in the *J-L-V* curves occurring at higher applied voltages. An operating voltage of about 4.3 V yields a brightness of 100 cd/m², 6.3 V yields 1,000 cd/m², and 9.8 V yields 10,000 cd/m². The luminescence reached ca. 36,700 cd/m² (at 17.0 V), which is comparable to that of a previously reported PHOLED device (Yang & Neher, 2004) made by spin-coating. Thus, it is clear that the proper adsorption of ions at the electrode surface can result in the formation of the ionic *p-i-n* structure and enhance the injection of charge carriers into the H-dip-coated organic layer, which results in the enhancement of current flow and EL luminance. In order to confirm the high performance of the sample devices, we also calculated the efficiency of the devices studied, as shown in Figure 12(b). For the H-dip-coated ionic *p-i-n* PHOLED, η_C of 3.0 cd/A was obtained at 100 cd/m², reaching η_C = 26.0 cd/A at 800 cd/m². We also calculated η_P of the H-dip-coated device, which reached a maximum of 13.6 lm/W. These results clearly indicated that the EL layer manufactured by H-dip-coating possesses bright and efficient EL characteristics due to the formation of a uniform layer with the appropriate ionic *p-i-n* structure.

Next, in order to check the processing ability of large-area ionic *p-i-n* PHOLEDs, we also fabricated a 10 × 10 cm² ionic *p-i-n* PHOLED device using the H-dipping process on an ITO-coated glass substrate. A photographic image of the fabricated device is shown in Figure 13. A PEDOT:PSS layer and an EL layer were deposited on a strip-patterned 10 × 10 cm² ITO-coated glass substrate by H-dipping, in order to fabricate a passive-matrix display device. The pixel array was 10 × 10 and the pixel size was 9 × 9 mm². It may be seen from the figure that the fabricated ionic *p-i-n* PHOLEDs were fairly luminous. The EL spectra were collected from each of the 100 individual pixels on the substrate, and were almost identical for each pixel, the emission peak wavelength being ~510 nm with a FWHM of about 70 nm. The

variation of the emitting intensity at different pixels was quite low. This result implies that the variation in the thickness of the organic thin film was small, because the EL intensity from a PHOLED is sensitive to the layer thickness. The low variation of EL intensity is quite acceptable for large-scale fabrication. These results confirm that the H-dipping method shows considerable promise for use in simple fabrication techniques that may easily be scaled up to a larger size at a lower cost than other processes. It should be noted that we were not able to form a homogeneous and uniformly thin EL layer by spin-coating for EL solutions on a 10 × 10 cm^2 substrate. From the results reported above, it is clear that the H-dipping process for solution coating shows considerable promise for the fabrication of bright and large-area ionic *p-i-n* PHOLEDs. It is worth noting that the performance of ionic *p-i-n* PHOLEDs may be further enhanced by, for example, the selection of more suitable materials, solvents, solution concentrations and viscosities, and by optimizing the gap height between the barrier and the substrate.

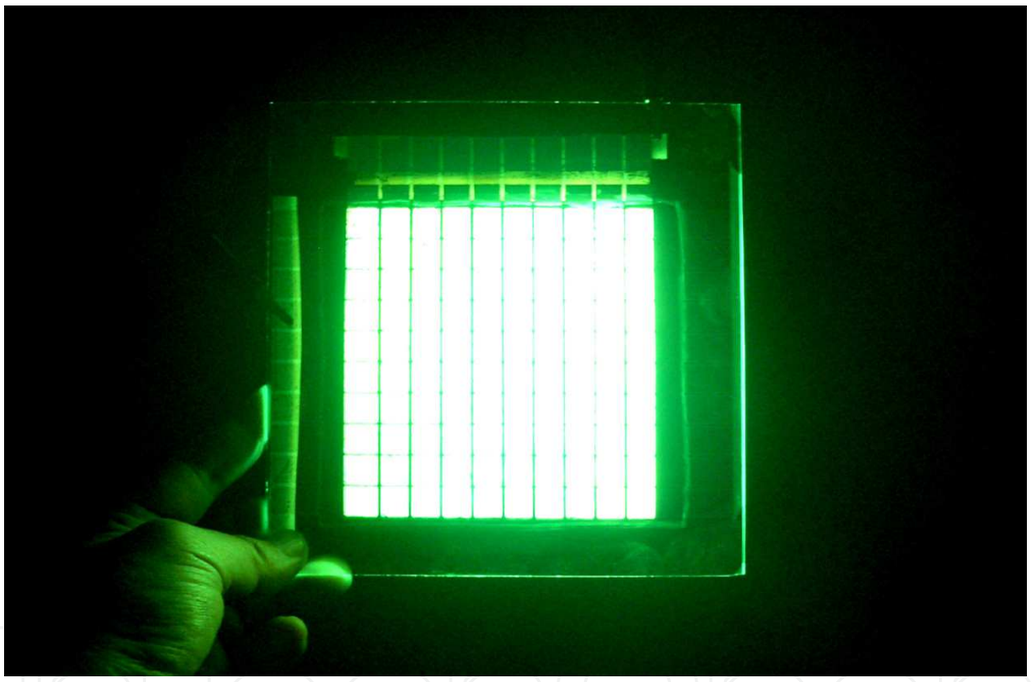

Fig. 13. A photograph of the operating 10 × 10 pixels of *p-i-n* PHOLEDs made by the H-dipping method at 15 V on a glass substrate (10 × 10 cm^2).

A simple premetered H-dipping process has been investigated as a promising organic thin-film coating process for the manufacture of cost-efficient and large-area ionic *p-i-n* PHOLEDs. Organic semiconducting thin films were fabricated successfully on a 10 × 10 cm^2 substrate with a high uniformity using H-dipping in a solution whose meniscus was controlled by adjusting the gap height and coating speed. It was also shown that bright and efficient ionic *p-i-n* PHOLEDs were produced. Experimental results indicate that the H-dipping method also shows great potential for applications involving large-area ionic *p-i-n* PHOLEDs. This novel process for depositing the solution on the substrate can be expanded to slot-die and slit-die coatings, and will provide a solid foundation for extending the fabrication of large-area solution processed PHOLEDs.

5. Summary

This chapter presented the fabrication and operation of the solution processed ionic *p-i-n* PHOLEDs. By applying the simultaneous electric and thermal treatments, homogeneous and enhanced EL emission with increased efficiency can be obtained from the devices in a simple fashion. Combining the simultaneous annealing process presented here with luminous organic materials will surely lead to the development of highly luminous large-area ionic *p-i-n* PHOLEDs, which will render the use of such devices possible for many applications, such as lighting, displays, and/or optoelectronic devices.

Acknowledgments

This research was supported by Basic Science Research Program through the National Research Foundation of Korea (NRF) funded by the Ministry of Education, Science and Technology (2010-0005557 and 2010-0016549). BP thanks Ms. M. Han and Mr. H. G. Jeon for their useful discussion at the early stage.

6. References

Adachi. C.; Thompson. M. E. & Forrest. S. R. (2002). Architectures for Efficient Electrophosphorescent Organic Light-Emitting Devices. *IEEE Journal on Selected Topics in Quantum Electronics*, vol. 8, no. 2, 372-7.

Baldo. M. A.; O'Brien. D. F.; You. Y.; Shoustikov. A.; Sibley. S.; Thompson. M. E. & Forrest. S. R. (1998). Highly efficient phosphorescent emission from organic electroluminescent devices. *Nature(London),* vol. 395, no. 6698, 151-4.

Baldo. M. A.; Lamansky. S.; Burrows. P. E.; Thompson. M. E. & Forrest. S. R. (1999). Very high-efficiency green organic light-emitting devices based on electro-phosphorescence. *Applied Physics Letters*, vol. 75, no. 1, 4-6.

Brütting. W.; Berleb S. & Mückl. A. G. (2001). Device physics of organic light-emitting diodes based on molecular materials. *Organic Electronics,* vol. 2, no. 1, 1-36.

Burroughes. J. H.; Bradley. D. D. C.; Brown. A. R.; Marks. R. N.; Mackay. K.; Friend. R. H.; Burns. P. L. & Holmes. A.B. (1990). Light-Emitting diodes based in conjugated polymer. *Nature,* vol. 347, no. 6301, 539-541.

Burrows. P. E. & Forrest. S. R. (1994). Electroluminescence from trap-limited current transport in vacuum deposited organic light emitting devices. *Applied Physics Letters,* vol. 64, no. 17, 2285-7.

Chason. E.; Picraux. S. T.; Poate. J. M. & Borland. O. (1997). Ion beams in silicon processing and characterization. *Journal of Applied Physics,* vol. 81, no. 10. 6513-6562.

de Gans. B.-J.; Duineveld. P. C. & Schubert. U. S. (2004). Inkjet Printing of Polymers: State of the Art and Future Developments. *Advanced Materials,* vol. 16, no. 3, 203-213.

de Mello. J. C.; Tessler. N.; Graham. S. C. & Friend. H. (1998). Ionic space-charge effects in polymer light-emitting diodes. *Physical Review B,* vol. 57, no. 20, 12951-12963.

Duffy. C. M.; Andreasen. J. W.; Breiby. D. W.; Nielsen. M. M.; Ando. M.; Minakata. T. & Sirringhaus. H. (2008). High-Mobility Aligned Pentacene Films Grown by Zone-Casting. *Chemistry of Materials,* vol. 20, no. 23, 7252–9.

Friend. R. H.; Gymer. R. W.; Holmes. A. B.; Brroughes. J. H.; Marks. R. N.; Taliani. C.; Bradly. D. D. C.; Dos Santos. D. A.; Bredas. J. L.; Logdlund. M. & Salaneck. W. R. (1999). Electroluminescence in conjugated
polymers. *Nature,* vol. 397, no. 6715, 121-8.

Gao. J.; Yu. G. & Heeger. A. J. (1997). Polymer light-emitting electrochemical cells with frozen *p-i-n* junction. *Applied Physics Letters*, vol. 71, no. 10, 1293-5.

Gerstner. E. G.; Cheong. T. W. D. & Shannon. J. M. (2001). Formation of bulk unipolar diodes in hydrogenated amorphous silicon by ion implantation. *IEEE Electron Device Letters,* vol. 22, no. 11, 536-8.

He. G.; Pfeiffer. M.; Leo. K.; Hofmann. M.; Birnstock. J.; Pudzich. R. & Salbeck. J. (2004). High-efficiency and low-voltage *p-i-n* electrophosphorescent organic light-emitting diodes with double-emission layers. *Applied Physics Letters,* vol. 85, no. 17, 3911-3.

Jabbour. G. E.; Radspinner. R. & Peyghambarian. N. (2001). Screen Printing for the Fabrication of Organic Light-Emitting Devices. *IEEE Journal on Selected Topics in Quantum Electronics*, vol. 7, no. 5, 769-773.

Krozel. J. W.; Palazoglu. A. N. & Powell. R. L. (2000). Experimental observation of dip-coating phenomena and the prospect of using motion control to minimize fluid retention. *Chemical Engineering Science,* vol. 55, no. 18, 3639-3650.

Kuo. C.-C.; Payne. M. M.; Anthony. J. E. & Jackson. T. N. (2004). TES Anthradithiophene Solution-Processed OTFTs with 1 cm^2/V-s Mobility, *2004 International Electron Device Meeting Technical Digest*, 373-6.

Landau. L. D. & Levich. V. G. (1942). Dragging of a liquid by a moving plate. *Acta Physicochimica URSS*, vol. 17, 42-54.

Lee. T. W.; Lee. H. C. & Park. O. O. (2002). High-efficiency polymer light-emitting devices using organic salts: A multilayer structure to improve light-emitting electrochemical cells. *Applied Physics Letters*, vol. 81, no. 2, 214-7.

Liu. H.-M.; He. J.; Wang. P.-F.; Xie. H.-Z.; Zhang. X.-H.; Lee.C.-S. & Xia.Y.-J. (2005). High-efficiency polymer electrophosphorescent diodes based on an Ir (III) complex. *Applied Physics Letters*, vol. 87, no. 22, 221103-5.

Luurtsema. G. A. (1997). Spin coating for rectangular substrates. U.Califonia, Berkely, [Online]. Available: http://bcam.berkeley.edu/ARCHIVE/theses/gluurtsMS.pdf.

Miskiewicz. P.; Mas-Torrent. M.; Jung J.; Kotarba. S.; Glowacki. I.; Gomar-Nadal. E.; Amabilino. D. B.; Veciana. J.; Krause. B.; Carbone. D.; Rovira. C. & Ulanski. J. (2006). Efficient High Area OFETs by Solution Based Processing of a pi-Electron Rich Donor. *Chemistry of Materials,* vol. 18, no. 20, 4724-9.

Niu. Y. –H.; Ma. H.; Xu. Q. & Jen. K.-Y. (2005). High-efficiency light-emitting diodes using neutral surfactants and aluminum cathode. *Applied Physics Letters*, vol. 86, no. 8, 083504-6.

Okamoto. S.; Tanaka. K.; Izumi. Y.; Adachi. H.; Yamaji. T. & Suzuki. T. (2001). Simple Measurement of Quantum Efficiency in Organic Electroluminescent Devices. *Japanese Journal of Applied Physics,* vol. 40, no. 7B, L783-4.

Ouyang. J.; Guo. T. –F.; Yang. Y.; Higuchi. H.; Yoshioka. M. & Nagatsuka. T. (2002). High-Performance, Flexible Polymer Light-Emitting Diodes Fabricated by a Continuous Polymer Coating Process. *Advanced Material,* vol. 14, no. 12 , 915-918.

Pardo. D.A.; Jabbour. G. E. & Peyghambarian. N. (2000). Application of Screen Printing in the Fabrication of Organic Light-Emitting Devices. *Advanced Material,* vol. 12, no. 17, 1249-1252.

Park. B. & Han M. (2009). Photovoltaic characteristics of polymer solar cells fabricated by pre-metered coating process. *Optics Express*, vol. 17, no. 16, 13830-13840.

Park. J. H.; Oh. S. S.; Kim. S. W.; Choi. E. H.; Hong. B. H.; Seo. Y. H.; Cho. G. S. & Park. B. (2007). Double interfacial layers for highly efficient organic light-emitting devices. *Applied Physics Letters,* vol. 90, no. 15, 153508-1-3.

Pei. Q.; Yu. G.; Zhang. C.; Yang. Y. & Heeger. A. J. (1995). Polymer Light-Emitting Electrochemical Cells. *Science,* vol. 269, no. 5227, 1086-8.

Sakuratani. Y.; Asai. M.; Tokita. M. & Miyata. S. (2001). Enhanced electron injection and electroluminescence in poly(*N*-vinyl carbazole) film doped with ammonium salt. *Synthetic. Metals,* vol. 123, no. 2, 207-210.

Suzuki. M.; Tokito. S.; Sato. F.; Igarashi. T.; Kondo. K.; Koyama. T. & Yamaguchi. T. (2005). Highly efficient polymer light-emitting devices using ambipolar phosphorescent polymers. *Applied Physics Letters*, vol. 86, no. 10, 103507-9.

So. F.; Krummacher. B.; Mathai. M. K.; Poplavskyy. D.; Choulis. S. A. & Choong. V. –E. (2007). Recent progress in solution processable organic light emitting devices. *Journal of Applied Physics,* vol. 102, no. 9, 091101-1-21.

Tang. C. W. & Van Slyke. S.A. (1987). Organic electroluminescent diodes. *Applied Physics Letters*, vol. 51, no. 12, 913-5.

Tseng. S. –R.; Meng. H. –F. & Lee. S. –F. (2008). Multilayer polymer light-emitting diodes by blade coating method. *Applied Physics Letter,* vol. 93, no. 15, 153308-1-3.

Xie. H. Z.; Liu. M. W.; Wang. O. Y.; Zhang. X. H.; Lee. C. S.; Hung. L. S.; Lee. S. T.; Teng. P. F.; Kwong. H. L.; Zheng. H. & Che. C. M. (2001). Reduction of Self-Quenching Effect in Organic Electrophosphorescence Emitting Devices via the Use of Sterically Hindered Spacers in Phosphorescence Molecules. *Advanced Materials,* vol. 13, no. 16, 1245-1248.

Xu. H.; Meng. R.; Xu. C.; Zhang. J.; Hee. G. & Cui. Y. (2003). A monolayer organic light-emitting diode using an organic dye salt. *Applied Physics Letters*, vol. 83, no. 5, 1020-2.

Yabu. H. & Shimomura. M. (2005). Preparation of self-organized mesoscale polymer patterns on a solid substrate: Continuous pattern formation from a receding meniscus. *Advanced Functional Materials,* vol. 15, no. 4, 575-581.

Yang. X. H. & Neher. D. (2004). Polymer electrophosphorescence devices with high power conversion efficiencies. *Applied Physics Letter,* vol. 84, no. 14, 2476-8.

Yim. Y. C.; Park. J. H.; Kim. S. W.; Choi. E. H.; Gho. G. S.; Seo. Y. H.; Kang. S. O.; Park. B.; Cho. S. H.; Kim. I. T.; Han. S. H.; Lim. J. & Takezoe. H. (2006). Enhanced light emission from one-layered organic light-emitting devices doped with organic salt by simultaneous thermal and electrical annealing. *Applied Physics Letters*, vol. 89, no. 10, 103507-9.

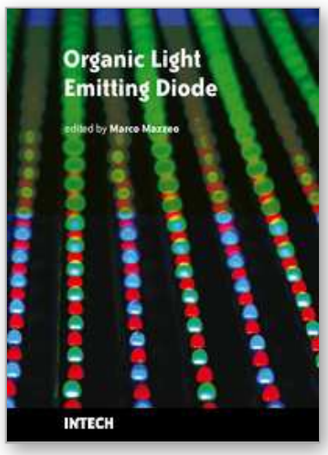

Organic Light Emitting Diode

Edited by Marco Mazzeo

ISBN 978-953-307-140-4
Hard cover, 224 pages
Publisher Sciyo
Published online 18, August, 2010
Published in print edition August, 2010

Organic light emitting diodes (OLEDs) have attracted enormous attention in the recent years because of their potential for flat panel displays and solid state lighting. This potential lies in the amazing flexibility offered by the synthesis of new organic compounds and by low-cost fabrication techniques, making these devices very promising for the market. The idea that flexible devices will replace standard objects such as television screens and lighting sources opens, indeed, a new scenario, where the research is very exciting and multidisciplinary. The aim of the present book is to give a comprehensive and up-to-date collection of contributions from leading experts in OLEDs. The subjects cover fields ranging from molecular and nanomaterials, used to increase the efficiency of the devices, to new technological perspectives in the realization of structures for high contrast organic displays and low-cost organic white light sources. The volume therefore presents a wide survey on the status and relevant trends in OLEDs research, thus being of interest to anyone active in this field. In addition, the present volume could also be used as a state-of-the-art introduction for young scientists.

INTECH
open science | open minds

InTech Europe
University Campus STeP Ri
Slavka Krautzeka 83/A
51000 Rijeka, Croatia
Phone: +385 (51) 770 447
Fax: +385 (51) 686 166
www.intechopen.com

InTech China
Unit 405, Office Block, Hotel Equatorial Shanghai
No.65, Yan An Road (West), Shanghai, 200040, China
中国上海市延安西路65号上海国际贵都大饭店办公楼405单元
Phone: +86-21-62489820
Fax: +86-21-62489821

IntechOpen